Scalable Computing: Practice and Experience, ISSN 1895-1767, http://www.scpe.org
© 2024 SCPE. Volume 25, Issues 4, pp. 2862–2875, DOI 10.12694/scpe.v25i4.2854

APPLICATION OF BIM TECHNOLOGY IN STRUCTURAL DESIGN OF PREFABRICATED BUILDING BASED ON BIG DATA SIMULATION MODELING ANALYSIS

LILI XU*, LIN WANG, AND MINMIN ZHU

Abstract. Aiming at the complex steel bar layout problem in prefabricated building, this research proposes a structural design method of prefabricated building based on big data simulation modeling building information modeling technology. It includes the reinforcement arrangement model based on agent path planning, the intelligent reinforcement arrangement of frame based on artificial potential field method and path optimization, and the modeling of Building information modeling. When analyzing the reinforcement arrangement effect of beam column joints in Prefabricated building, the calculation time of top corner joints is the shortest, 76.8 seconds, while that of middle layer joints is the longest, 141.7 seconds. In direction Y and direction X, differential evolution has the longest calculation time, 27s and 26.57s respectively, while particle swarm optimization algorithm has the shortest calculation time, 2.84s and 3.02s respectively. The algorithm designed through research is significantly superior to other algorithms in terms of computational time. In general, through building information modeling technology and big data simulation modeling, this study realized the collision free layout of rebar in beam column joints of prefabricated building. This improves the speed and efficiency of deepening design, and provides a new solution for structural design of prefabricated building.

Key words: Big data; BIM; Prefabricated; Building structure

1. Introduction. Computer technology has led to the widespread application of Big data (BD) intelligent algorithm technology in various industries such as industry and agriculture, resulting in improved industry efficiency and the construction industry benefiting from this. The traditional engineering construction model usually involves the design and construction of buildings being independently completed by different units. The design party formulates a design plan to guide the construction party in carrying out construction [1, 2, 3]. Construction drawings are one of the important ways to present design proposals. As the main communication medium during the construction process, their precision directly affects the quality, speed, and cost of actual construction. Therefore, the deep integration of architectural design with digital technology and intelligent methods is of great significance for promoting the high-quality development of intelligent construction [4, 5, 6]. However, due to increasingly stringent design cycle requirements, engineers often do not have enough time to consider the details of the solution. In addition, excessive manual input is difficult to ensure corresponding output improvement, resulting in a low level of design deepening. Especially evident in reinforced concrete structures, the design and construction of steel bars are closely related to the overall quality of the project [7, 8, 9]. Prefabricated building (PB) steel bar designs mostly only provide reinforcement schemes. Engineers consider multiple factors based on the calculation results of the steel bars and manually complete the reinforcement work, which has the problems of large calculation amount, time-consuming, and prone to errors. Therefore, intelligent design system based on BD is essential. The study first introduced the research purpose and conducted a literature review. Secondly, a PB structure strategy based on BD simulation modeling and BIM technology was designed. Then, data testing was conducted on the designed strategy. Finally, a conclusion was drawn.

2. Related works. In recent years, research on PB has been deepening year by year. Xiao Y's team explored the application of Building Information Modeling (BIM) technology in PB design and its comparison with traditional design methods, as well as the effectiveness verification of BIM collaborative design. A conceptual model for PCP collaborative design was established in the study, and the accuracy of BIM models at different design stages was determined. The effectiveness of the BIM based building collaborative design

*College of Engineering Cost, Zhejiang College of Construction, Hangzhou 311231, China (zjjylily@126.com).

method has been verified in examples [10]. Wasim M's team has comprehensively updated the integrated design, manufacturing, and assembly methods, and commented on their applications in the manufacturing and prefabrication fields. The writing of the comments followed slight modifications to the review of the preferred reporting system and the meta-analysis guidelines. There is a practical comparative relationship between prefabrication and manufacturing [11]. Wasim M uses an example of a volumetric steel structure to explore the integration of structural design and manufacturing assembly design (DfMA). DfMA principle can significantly improve the design efficiency of volumetric steel structures, enhance safety, sustainability, and production efficiency, while reducing costs and time [13]. Lee PC's team used MediaWiki to connect knowledge items with relevant BIM components, thereby expanding the knowledge ontology embedded in BIM. The proposed knowledge sharing platform and learning community model embedded in BIM have a positive impact on learning outcomes [13]. El Abidi K M A's team has revised the general motivations and limitations of PB in the construction industry. Research has found that the adaptability of PB is mainly influenced by factors such as labor shortage, labor costs, housing demand, construction process efficiency, climate conditions, and reducing waste materials and energy consumption. Although PB has inherent advantages in economy, environment, and social welfare, its application rate in the global construction industry is relatively low [14]. BIM technology application is gradually becoming more widespread. Matniyazov Z E's team studied the potential of BIM technology in solving modern design and construction industry problems. Their article carefully analyzed the problems and shortcomings of modern design technology in Uzbekistan, and further elaborated on the reasons for these problems through examples. After in-depth study, professionals will be able to understand why our economy needs new technologies [15]. Abdulmutalibovich K A's team conducted a detailed study of these competency characteristics and emphasized the effectiveness of the widespread application of modern information technology in enhancing architects' professional abilities. In addition, the advantages of fully developed professionals in solving complex problems were emphasized [16]. Xiao Y's team studied and compared BIM collaborative design with traditional design methods to promote the application of BIM in PB design. Based on the requirements of BIM technology IDM, a conceptual model of PCP collaborative design was established. The BIM based building collaborative design method has been validated in practice for its effectiveness [10]. Martins S S aims to explore the challenges faced by the application of integrated technology in 4D BIM in Brazil, a developing country, and verify them through Case study. He demonstrated the feasibility and challenges of using BIM technology to enhance communication between teams and stakeholders through visual presentation at different stages of construction [18]. In summary, the potential of BIM technology in solving modern design and construction industry problems, as well as its effectiveness in enhancing architects' professional abilities, has also been confirmed. However, BIM technology application in PB still faces many challenges. Therefore, this study will analyze BIM technology application in PB structure design based on BD simulation modeling, to improve the design efficiency and quality of PB.

3. PB Structure Design Based on BD Simulation Modeling and Analysis BIM Technology. This study aims to establish a reinforcement layout model based on intelligent agent (IA) path planning to achieve collision free arrangement of reinforcement in beam column nodes. And the original high-dimensional optimization task is decomposed into multiple low-dimensional optimization subtasks using a step-by-step optimization method that combines Artistic Potential Field (APF) and path planning. Finally, through secondary development of Revit software, a framework automatic deepening design plugin is created to improve the speed and efficiency of deepening design.

3.1. Intelligent Arrangement of Steel Bars in PB Beam Column Nodes Based on APF. In concrete beam column components, the main reinforcement generally includes two forms: longitudinal reinforcement and transverse reinforcement. When arranging steel bars, reserving space for hoops arrangement can avoid collisions between longitudinal bars and hoops. To achieve collision free layout of steel bars in beam column nodes, a steel bar layout model based on IA path planning will be established in the research. IA generally refers to any device or system that can autonomously perform complex tasks and can interact with humans through intelligent sensing devices. The IA path-planning-based rebar placement model is a method to optimize rebar placement using intelligent algorithms. In this model, the intelligent body represents an entity with autonomous decision-making capability, which is able to make decisions based on environmental information and its own state. Path planning is the core function of the intelligent body, which is used to

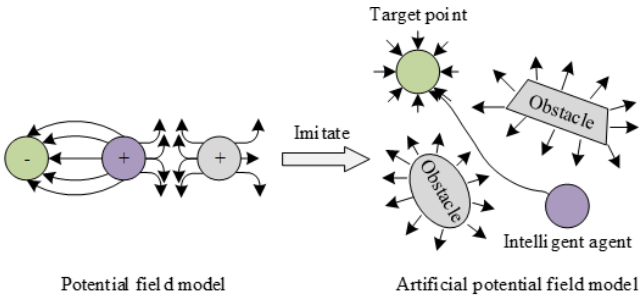

Fig. 3.1: Potential field model and artificial potential field model

determine its moving trajectory in the construction space. In order to ensure the accuracy and aesthetics of the rebar arrangement, the path obtained from the search is smoothed. After completing the path smoothing, the decision quality of the intelligent body is evaluated. The performance of the intelligent body is adjusted according to the evaluation results for more accurate path planning in subsequent construction. According to the optimized path, the intelligent body performs the placement of the steel bars. In this process, the intelligent body can dynamically adjust the scheduling program according to the actual situation to ensure the smooth progress of the construction process. In the process of steel bar arrangement, the deviation between the actual trajectory of the intelligent body and the planned path is monitored by the real-time monitoring system, and the path planning strategy of the intelligent body is adjusted in a timely manner if a large deviation is found in order to ensure the construction accuracy and safety. Through the above steps, the rebar placement model based on intelligent body path planning can realize the optimization of rebar placement, improve construction efficiency, and reduce the risk of manual intervention. In this model, beam column node is defined as the three-dimensional workspace of IA, and a local coordinate system is established with the bottom left corner of the column angle as the origin. X and Y axes are parallel to transverse and longitudinal beams, and Z axis is parallel to the vertical columns. For corner or edge nodes, after the reinforcement arrangement is completed, it is necessary to arrange the longitudinal reinforcement hooks of beam. In this process, a new IA needs to be placed at the end of the corresponding steel bar to ensure that the hook part of the steel bar does not collide with other steel bars.

APF is a path planning method based on the concepts of electric potential and electric field forces in physics, which guides IAs movement by establishing a virtual force field in the environment. APF has many advantages, such as simple computation, simple environmental modeling, and fast planning speed. Figure 3.1 shows the electric potential field model and the artificial potential field model.

One advantage of using APF for path planning is its simple calculation and implementation, making it easy to establish a mathematical model of the virtual potential energy field. According to the characteristics of the path planning task of IA, it is possible to choose to establish a Cartesian coordinate system in space or plane. In the reinforcement layout problem, the artificial potential field method can be used to guide the robot how to place the reinforcement. There are many specific parameters of the artificial potential field method. The potential field function defines the potential energy at each position in the environment. In general, the target location has a lower potential energy, while the obstacle or inaccessible area has a higher potential energy. The repulsive force coefficient determines the amount of repulsive force experienced by the robot. A larger repulsion coefficient will cause the robot to move away from the obstacle, while a smaller coefficient will make it easier for the robot to approach the obstacle. The coefficient of gravity determines the amount of attraction the robot receives. A larger gravitational coefficient will cause the robot to approach the target position faster, while a smaller coefficient will cause the robot to move more slowly. In some cases, obstacles or target locations in the environment may change as the robot moves. Therefore, it may be necessary to dynamically adjust the parameters of the potential field function to ensure that the robot can adapt to these changes. The application

of artificial potential field method to reinforcement layout problem is as follows. When laying out rebar, you can set the target point to where the rebar should be placed. For example, if you need to place a steel bar between two concrete walls, you can set the target point at the midpoint of the two walls. For rebar layout problems, repulsion functions can be defined to avoid collisions between rebar and walls or other rebar. For example, if a rebar is near a wall or another rebar, the repulsive force at that location can be increased, leading the robot to adjust its path. The gravity function is used to attract the rebar to move towards the target point. In this case, the target point is usually the intended location of the rebar. The speed and direction of rebar movement can be controlled by adjusting the parameters of gravity function. Equation 3.1 is to establish gravitational field $U_a(X)$ based on agent and target point's distance.

$$U_a(X) = \frac{1}{2} k \rho^2(X, X_g) \tag{3.1}$$

In equation 3.1, k is the gravitational coefficient. X and X_g are IA and target point's position vectors, respectively. $\rho(X, X_g)$ is IA and target point's distance. The farther agent is away from target point, the more gravitational energy will increase. On the contrary, it decreases. When the agent reaches target point, gravitational energy is usually 0. The gravity received by agent has a negative gradient relationship with gravitational field, so the gravity in formula 3.2 can be obtained by taking the derivative of gravitational field with respect to this distance

$$F_a(X) = -\nabla(U_a) = -k(X - X_g) \tag{3.2}$$

Equation 3.3 represents a repulsive field function of obstacles based on IA and target point's distance.

$$U_r(X) = \begin{cases} \frac{1}{2}\eta \left(\frac{1}{\rho(X, X_r)} - \frac{1}{\rho_0} \right)^2, & 0 \le \rho(X, X_r) \le \rho_0 \\ 0, & \rho(X, X_r) > \rho_0 \end{cases} \tag{3.3}$$

In equation 3.3, η is a repulsion coefficient, X_r is obstacle's position vector, $\rho(X, X_r)$ is IA and obstacle's distance, and ρ_0 is obstacle's influence range. The repulsion force and repulsion field received by IA also exhibit a negative gradient relationship. The repulsive force in equation 3.4 can be obtained by taking the derivative of repulsive force field with respect to distance.

$$F_r(X) = -\nabla(U_r) = \begin{cases} \eta \left(\frac{1}{\rho(X, X_r)} - \frac{1}{\rho_0} \right) \frac{1}{(\rho^2(X, X_r))} \frac{\partial \rho(X, X_r)}{\partial X}, & 0 \le \rho(X, X_r) \le \rho_0 \\ 0, & \rho(X, X_r) > \rho_0 \end{cases} \tag{3.4}$$

When there are multiple obstacles in the mobile environment, IA is in the total potential field of the superposition of gravitational potential field and multiple repulsive potential fields. Equation 3.5 calculates the total potential field.

$$U(X) = U_a(X) + \sum_{i=1}^{m} U_r^i(x) \tag{3.5}$$

In equation 3.5, m is obstacles number. The path planning of traditional APF has some limitations, which result in agent being unable to reach the target point in certain situations, leading to task failure. To solve the problem of unreachable target points near obstacles, the form of repulsive potential function is optimized by introducing the square of gent and target point's distance as a product term in repulsive potential function. The improved repulsive potential function ensures that target point is always the global minimum point of total potential energy field in equation 3.6.

$$U_r'(X) = \begin{cases} \frac{1}{2}\eta \left(\frac{1}{\rho(X, X_r)} - \frac{1}{\rho_0} \right)^2 \rho^2(X, X_g), & 0 \le \rho(X, X_r) \le \rho_0 \\ 0, & \rho(X, X_r) > \rho_0 \end{cases} \tag{3.6}$$

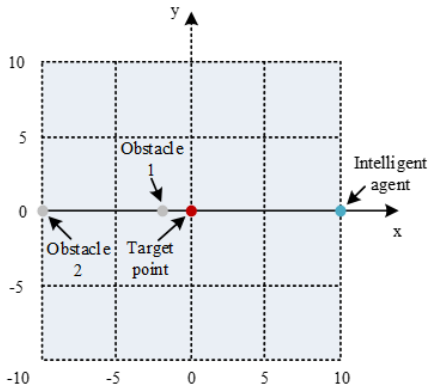

Fig. 3.2: 2D mobile environment

According to the value requirements of introducing the product term and graphic characteristics of Gaussian function, a deformed Gaussian function $G(X)$ is introduced as repulsion potential function's product term. Introducing $G(X)$ as original repulsive potential function's product term, a new repulsive potential function in equation 3.7 is obtained.

$$U_r''(X) = \begin{cases} \frac{1}{2}\eta\left(\frac{1}{\rho(X,X_r)} - \frac{1}{\rho_0}\right)^2\left(1 - e^{-\left(\frac{\rho^2(X,X_g)}{R^2}\right)}\right), & 0 \le \rho(X,X_r) \le \rho_0 \\ 0, & \rho(X,X_r) > \rho_0 \end{cases} \tag{3.7}$$

In equation 3.7, R is a radius of IA. Introducing $G(X)$ can effectively improve the distortion problem of total potential energy field far from target point. However. In some cases, the total potential field near target point may exhibit local minimum points. In this case, IA may stop or oscillate repeatedly, unable to ultimately reach the target point, as shown in Figure 3.2.

To eliminate the local minimum point of total potential energy field caused by obstacles near target point, this study will further reduce its value near target point by improving , and ensure that the value away from target point approaches 1. Therefore, a parameter β is introduced into $G(X)$, and a new form of Gaussian function $G_1(X)$ is proposed. The improved repulsive potential function in equation (8) is proposed by introducing $G_1(X)$ as a product term of repulsive potential function.

$$U_{r1}(X) = \begin{cases} \frac{1}{2}\eta\left(\frac{1}{\rho(X,X_r)} - \frac{1}{\rho_0}\right)^2\left(1 - e^{-\left(\frac{\rho^2(X,X_g)}{\beta R^2}\right)}\right), & 0 \le \rho(X,X_r) \le \rho_0 \\ 0, & \rho(X,X_r) > \rho_0 \end{cases} \tag{3.8}$$

By adjusting parameter β , the improved total potential energy field does not have a local minimum point near target point.

4. Intelligent Layout and BIM Modeling of Frame Reinforcement Based on APF and Path Optimization. APF is mainly aimed at solving the reactivity of IAs in mobile environments, making it difficult to optimize the mobile path. In the case of a large and densely distributed number of obstacles, IA may be affected by multiple obstacles at the same time, and may easily fall into local minimum points and stop moving, resulting in the inability to complete path planning. Therefore, when dealing with the problem of steel bar layout in complex environments, an intelligent steel bar layout model should be used to construct the mobile environment of IA, and a global optimization model for path planning should be established.

Global optimization of path planning is an important concept, especially in complex construction environments such as steel bar layout problems. The parameters of global path planning can be adjusted according to

the specific application and requirements to achieve the best performance. A global path is the complete path from the start to the end. The cost function is used to evaluate each possible path. In the case of reinforcement layout issues, this may include considering factors such as construction difficulty, time, material use, etc. In many practical applications, the environment is dynamically changing. Path planning requires the ability to identify and avoid obstacles. In a rebar layout, this may include walls, other rebar, or other physical barriers. The update frequency of global path planning determines the response speed of the planner to environmental changes. Faster update frequency means faster response, but it can also lead to unnecessary computational burden. The application of global optimization of path planning to reinforcement layout problem is as follows. In rebar layout, global path planning is used to determine the best rebar laying sequence and path. The optimal construction path is selected by considering a variety of factors, such as avoiding collisions with other steel bars and maximizing the efficiency of material use.

The task of global optimization in path planning is for an IA to find a collision free shortest moving path given a starting point and target point. The mobile path is represented by location points coordinates passed by IA, and entire mobile path is formed by connecting adjacent path points through a straight line. Assuming that there are a total D intermediate path points in the moving path of IA, except for the starting point and target point. The starting point coordinate of IA is $p_s = (x_0, y_0, z_0)$,, target point coordinate is $p_G = (x_(D+1), y_(D+1), z_(D+1))$, the -th intermediate path point coordinate is $p_i = (x_i, y_i, z_i)$, the path is represented as $p = (p_0, p_1, , p_D, p_(D+1))$, and $u_i = (u_(i, 1), u_(i, 2), u_(i, 3)) = (x_i - x_(i-1), y_i - y_(i-1), z_i - z_(i-1))$ represents the vector between adjacent two path points. Equation (9) represents each path point's coordinates.

$$\begin{cases} x_i = x_0 + \sum_{j=0}^{i} u_{j,1} \\ y_i = y_0 + \sum_{j=0}^{i} u_{j,2} \\ z_i = z_0 + \sum_{j=0}^{i} u_{j,3} \end{cases} \tag{4.1}$$

In order to reduce the search space and improve optimization efficiency, the step size of each movement of IA is limited to L_o , and equation 4.2 is adjacent two points' distance.

$$L_0 = \sqrt{u_{i,1}^2 + u_{i,2}^2 + u_{i,3}^2} \tag{4.2}$$

When arranging steel bars, steel bars bending usually occurs in lines rather than arcs. Therefore, in path planning, IA's movement direction is limited and can only move in directions parallel to three coordinate axes. This restriction ensures that two adjacent moving vectors are either perpendicular to each other or collinear to meet the specific constraint conditions in equation 4.3.

$$\begin{cases} u_{i,1} u_{i,2} = 0 \\ u_{i,1} u_{i,3} = 0 \\ u_{i,2} u_{i,3} = 0 \end{cases} \tag{4.3}$$

Assuming there are S intermediate path points in the moving path of IA, the binary variable dimension of the global path optimization solution is $3 * (D + 1)$. Figure 4 is an example of a global path optimization model solution using 15 dimensional binary encoding. There are 4 intermediate path points between starting and target points, and IA has made a total of 5 movements, moving once in positive direction. Then IA moves in positive direction, positive direction, negative direction, and finally moves in positive direction. Figure 4.1 shows the direction and order of IA's movement along the path.

For a moving path with d intermediate path points, it contains $d + 1$ moving vectors. The length of the overall path of an IA can be calculated by adding all motion vectors' lengths. To minimize agent's path length, an objective function l for global optimization of path planning in equation 4.4 is established.

$$\min L = \sum_{i=1}^{D+1} \sqrt{u_{i,1}^2 + u_{i,2}^2, u_{i,3}^2} \tag{4.4}$$

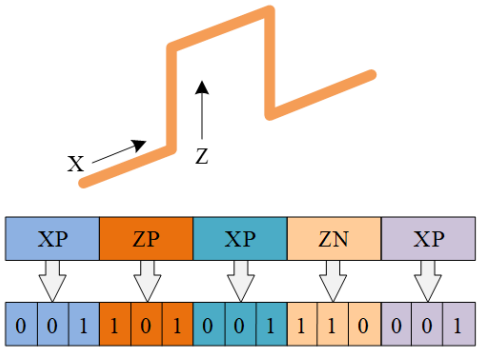

Fig. 4.1: Example of an agent path using binary encoding

When IAs moving, constraints such as collision and blockage of steel bars need to be considered. Considering the impact of constraint conditions on path planning results, a penalty function in equation 4.5 was established.

$$P_{po} = \begin{cases} +\infty, & \text{violation of constraints} \\ 1, & \text{others} \end{cases} \tag{4.5}$$

Penalty function is introduced into the path length and a fitness function for global optimization of path planning in equation 4.6 is constructed

$$\min F_g = P_{po} \cdot L \tag{4.6}$$

To ensure intelligent layout of steel bars' stability and efficiency, a step-by-step optimization method for path planning is studied. This method decomposes the original high-dimensional optimization task into multiple low-dimensional optimization subtasks, which can reduce optimization time and improve optimization success rate.

In the step-by-step optimization subtask, the position of sub target point cannot be predetermined, so sub path length cannot be used as path optimization model's objective function. To solve this problem, an objective function d in equation 4.7 can be established for each subtask by minimizing the distance between end point p_T^j and target point p_G .

$$\min d = \sqrt{(x_T^j - x_G)^2 + (y_T^j - y_G)^2 + (z_T^j - z_G)^2} \tag{4.7}$$

In this model, the constraints on steel collision and blockage are still considered, and a penalty function is introduced to establish a fitness function in equation 4.8.

$$\min F_d = P_{po} \cdot d \tag{4.8}$$

When obstacles are densely distributed, IA may encounter more types of obstacle forms, making it difficult to break away from local minimum points in Figure 4.2.

In Figure 4.3, placing two obstacles between IA and the target point generates two repulsive forces. When an IA moves to a certain point, repulsive force's magnitude is equal to gravitational force, causing agent to fall into a local minimum point. At the local minimum point formed by multiple obstacles, changing repulsive force's direction makes it difficult for agent to escape local minimum point.

APF can quickly calculate the next path point of the agent, but it is easily affected by the distribution of obstacles and may fall into local minimum points, leading to task failure. Path optimization methods can find the optimal path to ensure that agent reaches target point, but due to variable dimensions influence,

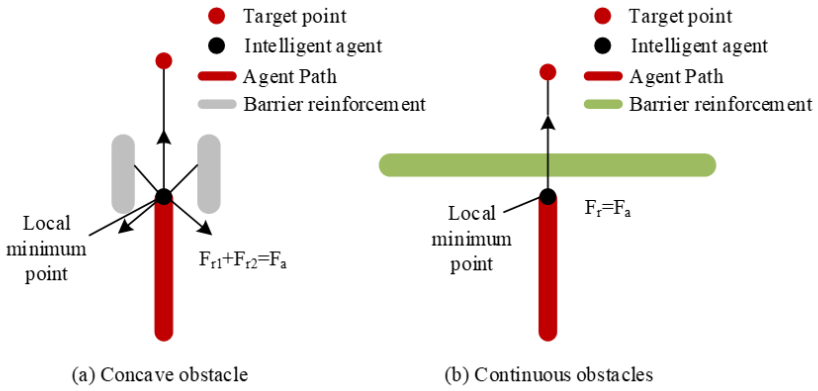

Fig. 4.2: The Local Minimum Problem of Artificial Potential Field Method in Complex Environments

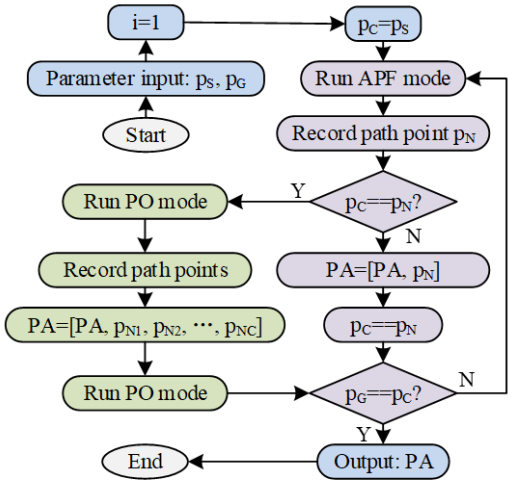

Fig. 4.3: The Path Planning Process of Hybrid Intelligent Method

optimization efficiency and quality may decrease. A hybrid intelligent method was proposed by combining the characteristics of APF and path optimization. Figure 4.3 shows a path planning of IAs based on hybrid intelligence methods [19, 20, 21].

Through secondary development of Revit software, a framework automatic deepening design plugin can be created to improve the speed and efficiency of deepening design. Revit secondary development is mainly carried out through application program interfaces, and external plugins are developed to extend Revit functionality. The plugin creates a class library project using Visual Studio software, writes code in C # language, and debugs this program to achieve intended functionality. Plugins can establish channels for transmitting data during design phase, create BIM models based on deepening design solutions, and automatically generate instances of elements such as beams, columns, and steel bars, thereby breaking the traditional mode of manual modeling. Figure 6 shows a deepening design process of PB framework.

5. Analysis on the Effect of Reinforcement Arrangement in PB Beams and Columns. This study conducted an effect analysis on the reinforcement arrangement of PB beam column joints. In the experiment, the calculation time of different types of nodes, the number of APF planning times, and the average

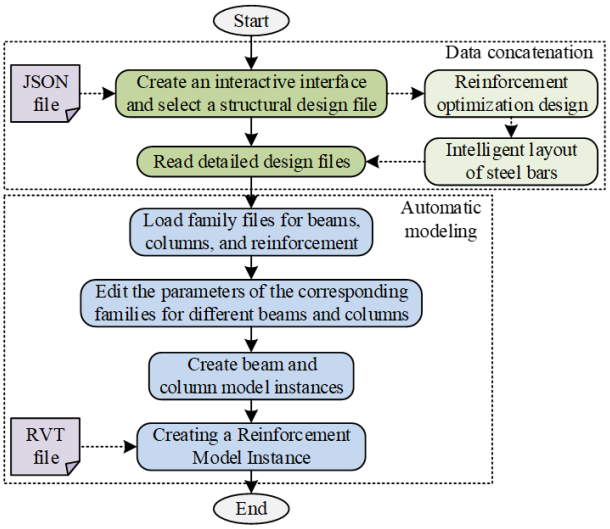

Fig. 4.4: Detailed design process of Prefabricated building frame

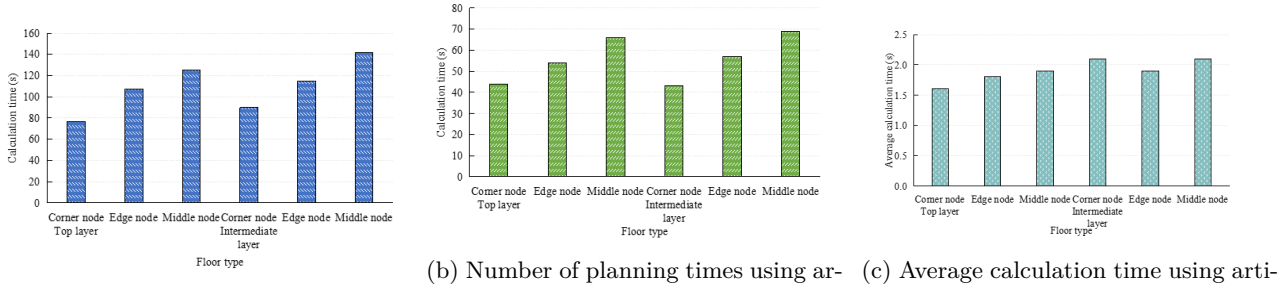

(a) Calculation Time

(b) Number of planning times using artificial potential field method

(c) Average calculation time using artificial potential field method

Fig. 5.1: Comparison of different node layout times

calculation time of APF were analyzed. The above analysis can reflect the differences in the difficulty of steel bar layout and computational complexity among different types of nodes. And a comparative analysis was conducted on the calculation time and path length of edge node beam reinforcement, middle node beam reinforcement, and corner node beam reinforcement in different directions.

5.1. Reinforcement Arrangement Effect Analysis of APF Prefabricated Building Beam Column Nodes. In this study, an improved APF was used to analyze the intelligent arrangement of steel bars in six different types of reinforced concrete beam column joints. These six types of nodes are: top corner, top edge, top middle, middle layer corner, middle layer edge, and middle layer middle nodes. Figure 5.1 shows the comparison of different nodes arrangement times.

Firstly, the calculation time of different types of nodes was compared and analyzed. The calculation time for the top corner node is the shortest, at 76.8 seconds, while the calculation time for the middle layer node is the longest, at 141.7 seconds. This may be because the structural complexity and difficulty of steel reinforcement arrangement of nodes in the middle layer are higher than other types of nodes, resulting in longer calculation time. Secondly, APF planning times for each type of node was compared. Among them, the planning times

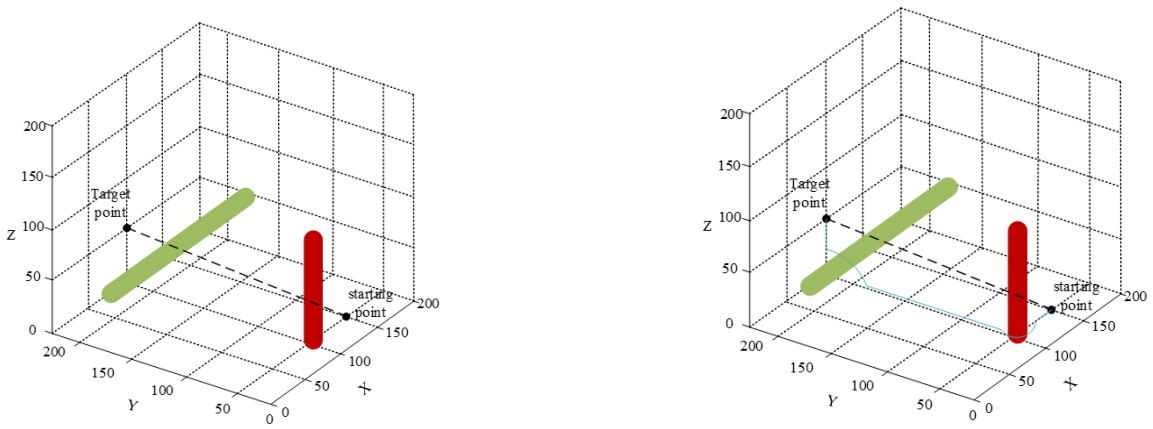

(a) Path Planning Task

(b) Path Panning Results

Fig. 5.2: 3D workspace of IAs

for the top layer corner nodes and the middle layer corner nodes are relatively low, with 44 and 43 times respectively. The nodes in the top layer and middle layer have more planning times, with 66 and 69 times respectively. This indicates that when using APF for steel reinforcement layout, the arrangement of middle nodes is more difficult and requires more planning times. In addition, the average calculation time for APF is relatively short, at 1.6 seconds and 2.1 seconds, respectively. Figure 8 shows the IA 3D workspace.

This study validated the feasibility of APF using a three-dimensional moving space as an example. To improve space utilization and ensure the safety of path planning, the impact range of obstacles is set to 1mm. Under this setting, IA successfully moved from the starting point to the target point under the guidance of APF, and the entire process took only 1.1 seconds. APF can effectively solve the problem of unreachable target points near obstacles.

5.2. Reinforcement Arrangement Effect Analysis in APF Prefabricated Building Framework. In 3D space, the calculation of the optimal path for IA is a challenging task, involving many factors such as spatial discretization, obstacle setting, selection of starting and target points, step size setting, and number of path points. In this example, the size of IA's moving space is a 1200mm × 1200mm × 600mm rectangular cuboid, and the space is discretized into a 1mm cube. Discretization makes the path planning problem can be accurately measured and solved. In this model, a steel bar located in Z direction is set as an obstacle, with the coordinates of its upper and lower position points being (600600600) and (600600, 0), respectively. Figure 5.3a shows the IA optimization path.

The starting point and target point coordinates of IA are (0, 600, 200) and (1200, 600, 200) respectively, with a step size of 20mm, and the middle points number in path is 70. These settings specify the movement range and stride fineness of IA, as well as path complexity. The algorithm designed through research can calculate a concise optimal path, which is effective. Figure 10 shows the algorithm calculation time.

From Figure 5.4, the scale and time consumption, iteration and time consumption are all proportional, withPSO algorithm taking the least time. Table 5.1 shows the calculation time and path length of edge node beam reinforcement for the research and design method.

In Table 5.1, DE algorithm has the longest calculation time in direction Y, which is 27 seconds. In contrast, PSO only takes 2.84 seconds, while NFO takes 8.58 seconds. This indicates that PSO has the highest computational efficiency. In direction X, DE algorithm requires 26.57 seconds, PSO requires 3.02 seconds, and NFO requires 8.63 seconds. PSO still has the highest computational efficiency. Through comparative analysis,

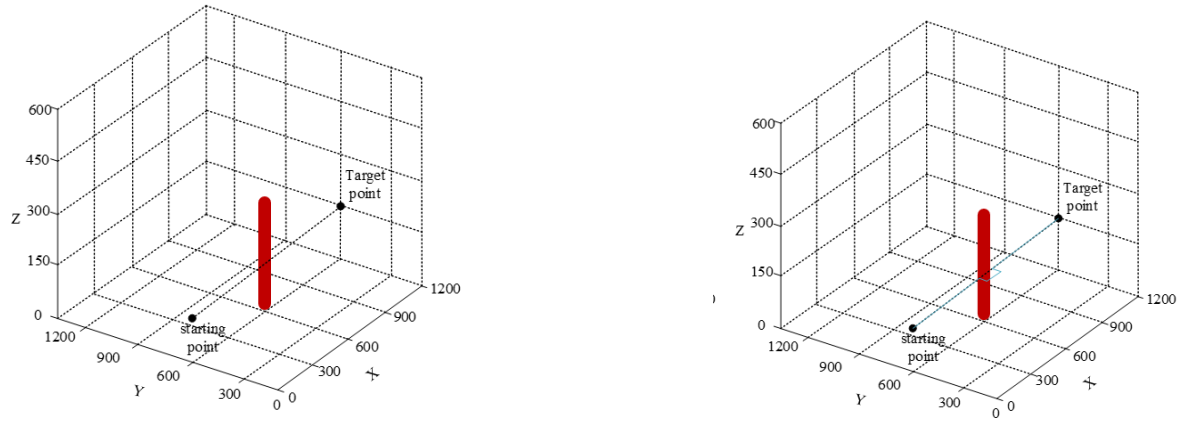

(a) 3D Workspace of intelligent Agents

(b) Optimal Path for Intelligent Agents

Fig. 5.3: Intelligent agent optimization path

Table 5.1: Calculation time and path length of edge node beam reinforcement

Direction	Position number	Length(mm)			Computing time(s)		
		DE	PSO	NFO	DE	PSO	NFO
Direction Y	1	1300	1300	1300	3.35	0.32	1.07
	2	1350	1350	1350	3.33	0.37	1.12
	3	1350	1350	1350	3.47	0.41	1.04
	4	1350	1350	1350	3.35	0.32	1.14
	5	1350	1350	1350	3.35	0.37	1.09
	6	1300	1300	1300	3.35	0.37	1.05
	7	1300	1300	1300	3.47	0.35	1.03
	8	1300	1300	1300	3.33	0.33	1.04
	Total	10600	10600	10600	27	2.84	8.58
DirectionX	1	1370	1370	1370	3.42	0.39	1.08
	2	1370	1370	1370	3.25	0.42	1.08
	3	1370	1370	1370	3.34	0.33	1.08
	4	1300	1300	1300	3.32	0.41	1.11
	5	1300	1300	1300	3.32	0.43	1.05
	6	1300	1300	1300	3.32	0.39	1.04
	7	1300	1300	1300	3.29	0.32	1.05
	8	1370	1370	1370	3.31	0.33	1.14
	Total	10680	10680	10680	26.57	3.02	8.63

although the performance of the three algorithms in path length is the same, PSO is significantly better than DE and NFO algorithms in computational time. Table 5.2 shows the calculation time and path length of steel bars in the middle node beam.

In direction Y, total calculation time of DE algorithm is 26.85 seconds, while the calculation time of PSO and NFO algorithms is 2.71 seconds and 6.72 seconds, respectively. Similarly, in direction X, total calculation time of DE algorithm is 24.53 seconds, while the calculation time of PSO and NFO algorithms is 2.66 seconds and 6.79 seconds, respectively. The calculation time of PSO is the shortest among all algorithms. Table 5.3 shows the calculation time and path length of corner node beam reinforcement.

In terms of path length, the path lengths of DE, PSO, and NFO algorithms remain consistent in both

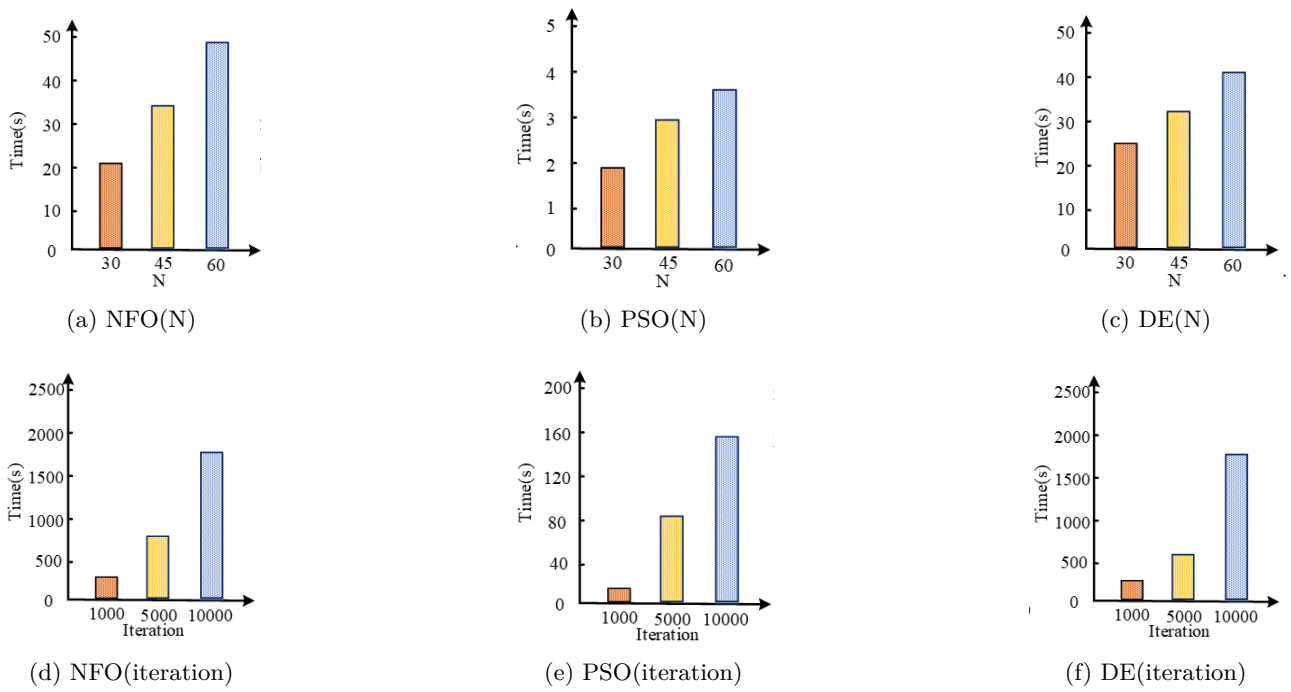

(a) NFO(N) (b) PSO(N) (c) DE(N)

(d) NFO(iteration) (e) PSO(iteration) (f) DE(iteration)

Fig. 5.4: Algorithm time comparison

Table 5.2: Calculation time and path length of steel bars in middle node beams

Direction	Position number	Length(mm)			Computing time(s)		
		DE	PSO	NFO	DE	PSO	NFO
DirectionY	1	1300	1300	1300	3.32	0.32	0.84
	2	1350	1350	1350	3.36	0.33	0.92
	3	1350	1350	1350	3.37	0.37	0.79
	4	1350	1350	1350	3.39	0.33	0.83
	5	1350	1350	1350	3.34	0.31	0.82
	6	1300	1300	1300	3.41	0.36	0.85
	7	1300	1300	1300	3.33	0.37	0.85
	8	1300	1300	1300	3.33	0.32	0.82
	Total	10600	10600	10600	26.85	2.71	6.72
DirectionX	1	1370	1370	1370	3.07	0.33	0.83
	2	1370	1370	1370	3.05	0.37	0.84
	3	1370	1370	1370	3.09	0.36	0.84
	4	1300	1300	1300	3.12	0.31	0.82
	5	1300	1300	1300	3.11	0.33	0.83
	6	1300	1300	1300	3.02	0.33	0.85
	7	1300	1300	1300	3.02	0.31	0.91
	8	1370	1370	1370	3.05	0.32	0.87
	Total	10680	10680	10680	24.53	2.66	6.79

Table 5.3: Calculation time and path length of corner node beam reinforcement

Direction	Position number	Length(mm)			Computing time(s)		
		DE	PSO	NFO	DE	PSO	NFO
DirectionY	1	1300	1300	1300	3.32	0.41	1.12
	2	1350	1350	1350	3.38	0.39	1.07
	3	1350	1350	1350	3.37	0.39	1.09
	4	1350	1350	1350	3.35	0.37	1.09
	5	1350	1350	1350	3.32	0.32	1.09
	6	1300	1300	1300	3.31	0.33	1.07
	7	1300	1300	1300	3.32	0.32	1.08
	8	1300	1300	1300	3.35	0.39	1.11
	Total	10600	10600	10600	26.72	2.92	8.72
DirectionX	1	1370	1370	1370	3.31	0.31	1.06
	2	1370	1370	1370	3.35	0.33	1.02
	3	1370	1370	1370	3.32	0.37	1.06
	4	1300	1300	1300	3.31	0.33	1.07
	5	1300	1300	1300	3.36	0.33	1.07
	6	1300	1300	1300	3.35	0.32	1.07
	7	1300	1300	1300	3.35	0.35	1.09
	8	1370	1370	1370	3.32	0.35	1.08
	Total	10680	10680	10680	26.67	2.69	8.52

directions Y and X. Specifically, the path length in direction Y is 1300mm or 1350mm, totaling 10600mm. The path length in direction X is 1300mm or 1370mm, totaling 10680mm. This indicates that three algorithms' performance in path optimization is equivalent, and they can complete the arrangement of corner node beam reinforcement within the same path length. However, these three algorithms exhibit significant differences in computational time. Both in direction Y and direction X, the calculation time of DE is the longest, reaching 26.72 seconds and 26.67 seconds. The calculation time of PSO is the shortest, only 2.92 seconds and 2.69 seconds. The calculation time of NFO is located in the middle, which is 8.72 seconds and 8.52 seconds, respectively. This indicates that under the same task, PSO has the highest computational efficiency, DE has the lowest computational efficiency, and NFO has a computational efficiency between these two.

6. Conclusion. This study conducts in-depth research on the collision free arrangement of steel bars in PB beam column joints by introducing BIM technology and combining BD simulation modeling analysis. Specifically, this study first proposes a reinforcement layout model based on IA path planning, and further proposes a framework reinforcement intelligent layout and BIM modeling method by combining APF and path optimization methods. The calculation time for the top corner node is the shortest, only 76.8 seconds, while the calculation time for the middle layer node is the longest, up to 141.7 seconds. Meanwhile, research has also found that different algorithms may have different efficiency when solving the same problem. Although the performance of DE, PSO, and NFO algorithms is consistent in terms of path length, PSO is significantly better than DE and NFO algorithms in terms of computational time. For example, for the edge node beam reinforcement in direction Y, the calculation time of PSO is only 2.84 seconds, while the calculation time of DE and NFO algorithms is 27 seconds and 8.58 seconds, respectively. This study achieved collision free arrangement of steel bars in PB beam column nodes, improving the speed and efficiency of deepening design.

Fundings. The research is supported by: The first batch of teaching reform projects in Zhejiang Province's vocational education during the 14th Five Year Plan period: Practical Research on the Implementation Path of the "Three Education Reform" Guided by Skills Competition under the Background of the "Double High" Construction (Project No.: jg20230176).

REFERENCES

[1] Wang, Y., Xue, X., Yu, T. & Wang, Y. Mapping the dynamics of China's prefabricated building policies from 1956 to 2019: A bibliometric analysis. *Building Research & Information*. **49**, 216-233 (2021)

[2] Sharma, S., Verma, K. & Hardaha, P. Implementation of artificial intelligence in agriculture. *Journal Of Computational And Cognitive Engineering*. **2**, 155-162 (2023)

[3] Ma, M., Zhang, K., Chen, L. & Tang, S. Analysis of the impact of a novel cool roof on cooling performance for a low-rise prefabricated building in China. *Building Services Engineering Research And Technology*. **42**, 26-44 (2021)

[4] Han, Y., Wang, L. & Kang, R. Influence of consumer preference and government subsidy on prefabricated building developer's decision-making: A three-stage game model. *Journal Of Civil Engineering And Management*. **29**, 35-49 (2023)

[5] Li, Z., Zhang, S., Meng, Q., Meng, Q. & Hu, X. Barriers to the development of prefabricated buildings in China: A news coverage analysis. *Engineering, Construction And Architectural Management*. **28**, 2884-2903 (2021)

[6] Wang, Y., Wang, F., Sang, P. & Song, H. Analysing factors affecting developers' behaviour towards the adoption of prefabricated buildings in China. *Environment, Development And Sustainability*. **23** pp. 14245-14263 (2021)

[7] Alkhalidi, A., Abuothman, A., AlDweik, A. & Al-Bazaz, A. Is it a possibility to achieve energy plus prefabricated building worldwide?. *International Journal Of Low-Carbon Technologies*. **16**, 220-228 (2021)

[8] He, W., Li, W. & Meng, X. Scheduling optimization of prefabricated buildings under resource constraints. *KSCE Journal Of Civil Engineering*. **25**, 4507-4519 (2021)

[9] Wang, Y. & Wang, Y. Research on the integration of bim technology in prefabricated buildings. *World Journal Of Engineering And Technology*. **9**, 579-588 (2021)

[10] Xiao, Y. & And, B. and optimization of prefabricated building system based on BIM technology. *International Journal Of System Assurance Engineering And Management*. **13** pp. 111-120 (2022)

[11] Wasim, M., Vaz Serra, P. & Ngo, T. Design for manufacturing and assembly for sustainable, quick and cost-effective prefabricated construction–a review. *International Journal Of Construction Management*. **22**, 3014-3022 (2022)

[12] Wasim, M. & Oliveira, O. Efficient design of a prefabricated steel structure integrating design for manufacture and assembly concepts. *Australian Journal Of Structural Engineering*. **23**, 356-369 (2022)

[13] Lee, P., Lo, T., Wen, I. & Xie, L. The establishment of BIM-embedded knowledge-sharing platform and its learning community model: A case of prefabricated building design. *Computer Applications In Engineering Education*. **30**, 863-875 (2022)

[14] El-Abidi, K. Ghazali F E M. *Motivations And Limitations Of Prefabricated Building: An Overview*. **802** pp. 668-675 (2015)

[15] Matniyazov, Z. & Buronov, N. Why Does A Project Organization Need Bim Technologies?. *Eurasian Journal Of Learning And Academic Teaching*. **13** pp. 17-20 (2022)

[16] Abdumutalibovich, K. & Lutfillaevna, B. The Role of Bim Technologies in the Information System of Education. *European Journal Of Contemporary Business Law & Technology: Cyber Law, Blockchain, And Legal Innovations*. **1**, 9-13 (2023)

[17] Xiao, Y. & And, B. and optimization of prefabricated building system based on BIM technology. *International Journal Of System Assurance Engineering And Management*. **13** pp. 111-120 (2022)

[18] Martins, S. Evangelista A C J, Hammad A W A, Tam V W Y, Haddad A. *Evaluation Of*. **22**, 2987-3000 (2022)

[19] Almusaylim, Z., Zaman, N. & Jung, L. Proposing a data privacy aware protocol for roadside accident video reporting service using 5G in Vehicular Cloud Networks Environment. *2018 4th International Conference On Computer And Information Sciences (ICCOINS)*. pp. 1-5 (2018)

[20] Humayun, M., Ashfaq, F., Jhanjhi, N. & Alsadun, M. Traffic management: Multi-scale vehicle detection in varying weather conditions using yolov4 and spatial pyramid pooling network. *Electronics*. **11**, 2748 (2022)

[21] Singhal, V., Jain, S., Anand, D., Singh, A., Verma, S., Rodrigues, J., Jhanjhi, N., Ghosh, U., Jo, O., Iwendi, C. & Others Artificial intelligence enabled road vehicle-train collision risk assessment framework for unmanned railway level crossings. *IEEE Access*. **8** pp. 113790-113806 (2020)

Edited by: Zhengyi Chai
Special issue on: Data-Driven Optimization Algorithms for Sustainable and Smart City
Received: Nov 15, 2023
Accepted: Jan 22, 2024